X-RAY DIFFRACTION LINE BROADENING IN SHOCK MODIFIED PYRITE

B. MOROSIN*, R.A. GRAHAM* and S.S. POLLACK**
*Sandia National Laboratories, Albuquerque, NM 87185
**Pittsburgh Energy Technology Center, Pittsburgh, PA 15236

Powder compacts of a commercially-available pyrite, FeS_2, have been subjected to controlled, quantitative high pressure shock loading at peak pressures from 7.5-22 GPa. The profiles of the x-ray diffraction lines have been examined to determine the reduction of the crystallite (domain) size and the introduction of residual microstrain due to defects and dislocations resulting from the transmission and interaction of the shockwave. Pyrite experience a surprisingly smaller profile broadening than observed for all other materials under similar shock conditions, suggesting a much more refractory character. Such small changes are consistent with low defect densities and with the relative low reaction activity (oxidation of sulfide to sulfate by humid air) observed on this material in complementary studies.

1. INTRODUCTION

Considerable data on shock-modified materials have demonstrated substantially altered and enhanced solid state reactivity, both during and after shock compression. These behaviors have been attributed to the introduction of large number of defects into the crystalline lattice as well as to a reduction in the crystallite size of the powders.[1] X-ray diffraction profile analysis has provided a means of determining both the residual lattice microstrain and coherent crystallite size resulting from such defects.

Pyrite is an important mineral found in my locations on earth, being familiar to most for its golden luster as well as beautifully faceted habits. Pyrite is also found in coal deposits. One possible beneficial use of pyrite was an attempt to use the mineral matter present as well as further additions as a catalyst for liquefaction of coals.[2] In fact, a further enhancement of such studies concerned use of shock-modified pyrite[3]; however, the chemistry involved proved too complex and suggested reaction products of the pyrite may have been the actual catalyst involved in the liquefaction process. On the other hand, removal of pyrite for coals used in steam generation is desirable for environmental reasons. It has been found that various samples of pyrite respond differently to froth flotation and agglomeration treatments used for its removal. Earlier studies showed coal-derived pyrites oxidize much more rapidly in humid air than others and that particle size alone was not responsible for the increased reactivity.[5] Lack of data correlating crystal imperfection with reactivity suggested such a study on naturally occurring pyrites[5]. The present study used the shock-compression process as a source for controlled defects in pyrite. This paper reports an x-ray profile analysis on such shock-modified pyrite.

2. EXPERIMENTAL

The pyrite powder used was a commercial non-coal-derived material, MCB, (available from VWR Scientific; mined in Missouri). This material exhibits a reasonably sharp x-ray diffraction pattern, typical of a material with a crystallite size approaching 2000 A, and, hence, was assumed to have negligible residual strain. This material served as our standard used to determine the instrumental broadening for our peaks (see "Profile Analysis" below).

The samples were subjected to controlled shock compression with the "Bear" explosive-loading fixtures[1]. The pyrite powder was pressed into compacts in place within copper capsules of the sample recovery system. The fixtures were then subjected to controlled, quantifiable, high-explosive shock-wave loading conditions. The capsules are designed to form an air-tight seal. After retrieval of the sealed copper capsules from the recovery fixtures, they are sawed and pressed open. The recovered powder was separated in samples with respect to location within the capsule and designated as either bulk or outer circumferential edge. Such samples were lightly ground to break up agglomerates, if present, before further characterization.

Quantification of pressure and temperature conditions within the compacts has been achieved with an extensive program of numerical simulation using a two-dimensional computer code that describes the pressure-temperature history as the shock-wave propagates in the sample[1].

Table I. Schedule of Experiments: MCB Pyrite

Experiment	Explosive[c]	Density[a]		Peak Pressure	Temp. °C[b]	
---	---	g/cm³	%	GPa	Bulk	Edge
34H906	Baratol	2.99	60	7.5	150	175
33H906	Comp B	2.99	60	17	325	500
38H906	Comp B	2.50	50	17	475	575
39H906	Comp B	2.50	50	22	475	700

[a]Sample powder compact density
[b]Mean bulk shock temperature see text and ref. 1.
[c]Momma Bear fixture used only.

Various pressure and temperature pulses usually are obtained by varying the fixture size, explosive configuration, and initial packing density of the powder; however, in the present case, the fixture was identical for all experiments since sample size was important. For this reason, the higher pressures usually investigated were not carried out. These conditions are detailed in the schedule of shock-modification experiments as shown in Table I. The peak shock pressure varies from a value of 7.5 to 22 GPa, below the suggested 26 GPa transition in pyrite[6].

The peak profiles of the x-ray diffraction lines for pyrite were obtained with a Siemens automated diffractometer equipped with a monochromator on the detector set so that both α_1 and α_2 lines were collected. The aperture, divergent and receiving slits and the slits adjacent to the diffracted beam monochromator are all 0.1°. The intensity data were collected digitally with step increments of 2θ equal to 0.005°. Counting was done for fixed time (generally 20 seconds) while the beginning and final background points were counted for 200 seconds. Our counting statistics reflected requirements set upon the instrument for other uses and represents a compromise of several factors. The various (hkl) peaks examined are indicated below (in Figures 1 and 2).

3. PROFILE ANALYSIS

Our two recently developed computer codes[7] for analysis of broadened profiles are a profile fitting program, XRAYL, and a profile deconvolution and analysis program CRYSIZ. XRAYL allows the fitting of observed profiles which may consist of one or more diffraction lines by one of four mathematical functions, Gauss, Cauchy, Voight or Pearson VII. XRAYL produces smooth reference and broadened profiles corrected for background for use by CRYSIZ. XRAYL is particularly useful for separating diffraction lines which overlap in either the reference or on shock-modified samples with broadened lines. Another important feature is that the program provides the ability to force every unique line to cover the same span of 1/d space. A particular value of the variable a3, described by Warren[8], is selected to produce comparable background regions in 1/d space for all lines. We refer to this span as a "window." This program is ideal for carrying out computer modeling to ascertain the importance of various experimental and computational procedures employed on the raw profiles of the diffraction lines. Such modeling has confirmed the importance of obtaining fitted profiles which achieve a nominal "background" value on both sides; otherwise, serious errors will result in the subsequent calculations of size and strain values[7].

CRYSIZ carries out the steps necessary on the profiles from XRAYL to obtain the size and strain information. Such peaks may be those obtained by the mathematical functions or the natural data points augmented only with respect to the points describing the background in order to achieve the desired window. CRYSIZ deconvolutes the instrumental broadening by the usual Stoke's Fourier transform method[7]. The Fourier coefficients (free from instrumental broadening) are used for the subsequent steps to calculate the size and strain information using the Warren-Averbach (W-A) model as well as determining complimentary values by the traditional Hall-Williamson or Gauss-squared methods[7]. For these latter methods, we have employed the back Fourier transformed line, using the coefficients, corrected for instrumental broadening so as to have a line profile on which values of the full width at half maximum and second moment can be determined. Such values determined on the corrected line profiles can then be used for the traditional plotting methods as well as the usual multiple-line W-A procedure. Normally, the W-A procedure examines a particular x-ray line and its second order, e.g., (111) and (222), as a pair. Several such pairs were examined. In addition, the entire set of lines was treated as a single group resulting in an average with respect to all the observed lines. This is accomplished by treating them as a function of the square of the interplanar spacing rather than as the square of the index[7].

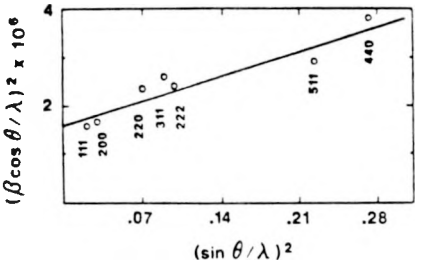

FIGURE 1

Gauss-squared plot for size and strain separation. β values are from second moments on back-transformed profiles. Sample is 33H906E.

4. RESULTS

Figure 1 shows the second moment data obtained on back Fourier transformed lines (instrumental broadening removed) on the edge portion of sample (33H906E). The least-squares line shown yields an intercept and slope corresponding to a Gauss-squared crystallite size D_G = 752 A and square-strain $e_G = 0.97 \times 10^{-3}$. Such values are usually different from those obtained by the W-A procedure as has been discussed by various authors[7,9].

Figure 2 shows a typical plot of the W-A Fourier coefficients as a function of the square of the reciprocal of the interplanar spacing, d. Data on sample 33H906E are shown for three values of L, where L is a distance along the perpendicular to the reflecting lattice planes (hkl) whose spacing is d. The straight lines through the particular L values correspond to a least-square line and the intercept would result in an "average" Fourier size coefficient while the slope would yield an "average" mean-square strain value. Correspondingly, a line through a particular line and its second (or higher) order would yield the corresponding information for that particular direction in the crystal.

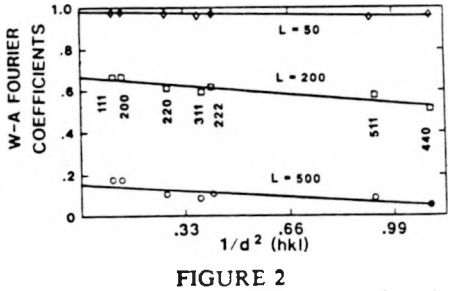

FIGURE 2

Warren-Averbach Fourier coefficients as a function of interplanar spacing for sample 33H906E. A least-squares line is show for each of three L values.

Table II. Size (A), D, and Strain ($x10^{-3}$), E

	111		110		Overall	
Samples[a]	D	E	D	E	D	E
34H906B	1090	0.29	996	0.38	1135	0.28
34H906E	942	0.27	923	0.34	1079	0.31
33H906E	546	0.45	523	0.53	576	0.50
38H906B	557	0.65	477	0.54	517	0.54
38H906E	576	0.65	521	0.65	552	0.60
39H906B	624	0.72	542	0.62	582	0.58
39H906E	555	0.67	464	0.68	514	0.65

[a]B designate "bulk"; E outer circumferential "edge".

By plotting either the size coefficients (intercepts for particular L values) or strain values (slopes) versus length L, one obtains curves from which information on the microstructure can be determined. From the size coefficient curve, by extrapolation at small L values, values of the W-A average area-weighted size <Da> may be obtained (Table II). Comparison of such size values shows an initial marked fall-off with increasing L values for intermediate shock pressures which corresponds to the reduction in size of the scattering domains with increasing pressure. This levels off towards higher pressures. Though we have only a limited pressure range, this behavior is similar to that observed in other materials previously studied and is indicative of post-shock annealing effects coming into play. This annealing effect is not as large as that determined for hematite, Fe_2O_3, another iron-containing mineral.[10] Figure 3 summarize the W-A size values as a function of shock pressure for pyrite and compares them with values for hematite.

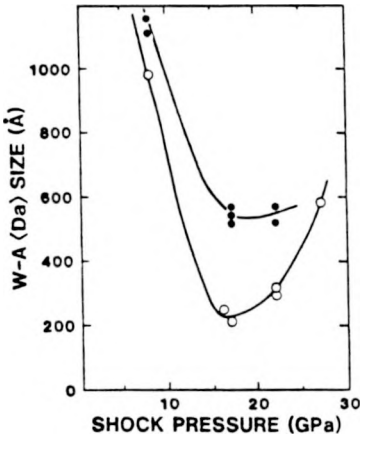

FIGURE 3

Warren-Averbach crystallite size versus shock pressure. Solid points are for pyrite; open hematite.

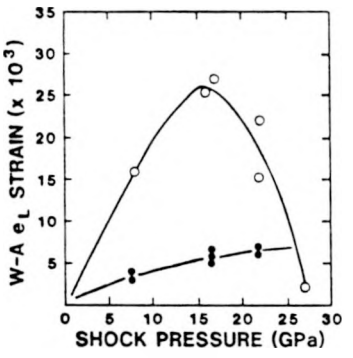

FIGURE 4

Warren-Averbach residual strain versus shock pressure. Solid points are for pyrite; open hematite.

Similarly, the corresponding root average mean square strain values as a function of L value show a rather gradual decrease in value as L increases. These values are not large, as could be predicted from the observation of the diffraction line widths; however, the general shape are typical of those for cold worked metals, of milled ceramics and of shock-modified materials. Such curves show that strains, averaged over short distances, are great and decrease or die out as they are averaged over larger coherent diffracting domains. By averaging such values of $\langle e^2(L) \rangle$ from 10 A to the appropriate $\langle Da \rangle$ size (Table II), a strain value, e_L, is obtained. These are summarized as a function of shock pressure in Fig. 4. Again, values are compared with those of hematite. Note that the strain values for pyrite are very much smaller, as predicted by visual inspection of the powder diffraction lines, than those for hematite. Nevertheless a slight dependence on shock pressure can be seen.

5. CONCLUDING REMARKS

The observed behavior is similar to that seen in some of our other shock-modified materials such as, besides hematite, rutile and TiC, namely, that a shock temperature effect occurs which causes the primary shock-pressure changes to be reversed[1]. The shock temperature may be controlled by varying the initial packing density of the sample, and, as it rises along with shock pressure, two effects on residual strain of recovered materials are observed. First in some hard refractories, more plastic deformation can occur under shock-loading when there is a higher shock temperature at the same mean peak shock pressure. Second, the effect of shock temperature may be sufficient for some materials to result in a post-shock annealing effect. The annealing effect is sufficient to reduce strain, increase crystallite size and reduce defect level concentrations as measured by other means, e.g., EPR, specific heat, and in present case, chemical reaction time.

Previous studies on various pyrites, including more reactive coal derived and museum specimens, showed a wide range of reactivity, determined by weathering materials at 0.98% relative humidity air moisture and observing conversion to the sulfate.[5] This reactivity rate scaled according to the dislocation density determined from the initial etch pit count on the samples. The MCB pyrite with 1.6×10^6 counts cm^{-2} was in the midrange for pyrites studied (2.6×10^5 to 6.4×10^8). Employing the sulfate/sulfide ratio as a measure of reactivity, ratio values were 0.16, 0.30, 0.33, and 0.05 for unshocked, 7.5 GPa, 17 GPa and 22 GPa samples, respectively. (A value of 0.93 for the most reactive sample studied from the Riverside coal mine in Queensland, Australia serves as a bench mark). These weathering studies are qualitatively consistent with the results obtained from the x-ray line profile analysis.

ACKNOWLEDGEMENTS

This work supported by the DOE under contract #DE-AC04-76DP00789.

REFERENCES

1. R. A. Graham, et al, Ann. Rev. Mater. Sci. 16 (1986) 315; references therein.
2. P. A. Montano, et al, Fuel 59 (1980) 214.
3. B. Morosin, et al, Appl. Phys. Comm. 5 (1985) 1; also see, Sandia Report SAND82-0658 (1983).
4. M. G. Thomas, et al, Fuel 61 (1982) 761.
5. S. S. Pollack, et al, Reactivity of Pyrites and Dislocation Densities, Proc. Int. Coal Conf. New Castle on Tyne, England, Sept. 1991.
6. T. J. Ahrens, J. Geophy. Res.84 (1979) 985.
7. Y. Zhang, et al, Adv. X-ray Anal. 33 (1990) 373; references therein.
8. B. E. Warren, Imperfect Crystals X-ray Diffraction (Addison-Wesley Menlo Park, CA 1969) Chapt 13.
9. R. Delhez, et al, Z. Anal Chem 312 (1982).
10. Y. Zhang, et al, Adv. X-ray Anal. 31 (1988) 287.